J Supercond Nov Magn (2011) 24:1767–1771
DOI 10.1007/s10948-010-1121-1

ORIGINAL PAPER

Room Temperature Magnetism in Co-doped ZnO Nanorods

Liguo Xu · Kai Shen · Qingyu Xu

Received: 7 December 2010 / Accepted: 21 December 2010 / Published online: 18 January 2011

Abstract $Zn_{1-x}Co_xO$ ($x = 0$, 0.02, 0.04, 0.06, 0.08, 0.10) nanorods have been synthesized by the hydrothermal method. XRD patterns show that all samples are wurtzite structure without impurity. The magnetization measurements show that the pure ZnO is diamagnetic, while paramagnetism dominates in $Zn_{1-x}Co_xO$ nanorods. Paramagnetism increases linearly with an increasing Co concentration. The magnetic moment calculated from the magnetic susceptibility is around 4 μ_B/Co, which is close to the theoretical value of Co ions with $L = 1.07$ and $S = 3/2$ in all $Zn_{1-x}Co_xO$ nanorods, indicating the Co atoms are mostly isolated. All the samples exhibit weak ferromagnetism. However, the saturation magnetization of the ferromagnetic contribution in $Zn_{1-x}Co_xO$ almost keeps constant with increasing Co concentration. We conclude that the weak ferromagnetism in $Zn_{1-x}Co_xO$ might be due to the high concentration of defects.

Keywords Diluted magnetic semiconductors · Co-doped ZnO · Ferromagnetism

1 Introduction

Recently, diluted magnetic semiconductors (DMS) with simultaneous control of charge and spin, have attracted intensive interests for the potential applications in spintronics [1]. For the daily applications, the Curie temperature should be higher than room temperature (RT). Dietl [2] has predicted the possible above RT ferromagnetism (FM) in Mn-doped p-type ZnO and GaN.

There have been already a lot of researches on ZnO-based DMS reporting the RT FM by doping with 3d transition metals [3, 4]. But various magnetic properties such as paramagnetism has also been found in the doped ZnO, thus the origin of FM is still under debate [5–8]. FM has been observed in Co-doped ZnO by superconducting quantum interference device (SQUID), but only the paramagnetic signal for Co ions observed by X-ray magnetic circular dichroism (XMCD) [9–11]. Thus, it is argued that the FM has to be attributed to the defects such as oxygen vacancy instead of the doped transition metal. In this paper, we prepared single phase $Zn_{1-x}Co_xO$ nanorods. Pure ZnO nanorods exhibit diamagnetism and $Zn_{1-x}Co_xO$ nanorods show paramagnetism, while weak FM has been observed in all samples. We conclude that most doped Co atoms in ZnO are isolated; the observed weak FM in $Zn_{1-x}Co_xO$ nanorods might be due to defects.

2 Experimental Details

$Zn_{1-x}Co_xO$ nanorods were synthesized by the hydrothermal method [12]. All chemicals are analytical grade (AR) and purchased from commercial sources without further treatment. In a typical procedure, 0.0015 mol of $Zn(NO_3)_2 \cdot 6H_2O$ and different mole ratios of $Co(NO_3)_2 \cdot 6H_2O$ were added into 30 ml absolute ethanol, and the solution was then subjected to magnetic stirring at RT for 0.5 h. 0.0075 mol NaOH was completely dissolved into 15 ml absolute ethanol with magnetic stirring, and the obtained solution was slowly

L. Xu · K. Shen (✉)
School of Materials Science and Technology,
Nanjing University of Aeronautics and Astronautics, Nanjing, 210016, China
e-mail: shenkai84@nuaa.edu.cn

Q. Xu
Department of Physics, Southeast University, Nanjing 211189, China

Table 1 The Co concentration measured by EDS and the lattice parameters calculated from the XRD data in $Zn_{1-x}Co_xO$ nanorods

Nominal Co concentration (%)		0	2	4	6	8	10
Co concentration measured by EDS (%)		0	1.8	3.6	4.9	6.7	10.1
Lattice constant (Å)	a	3.253	3.253	3.254	3.250	3.250	3.252
	c	5.211	5.211	5.205	5.207	5.211	5.198

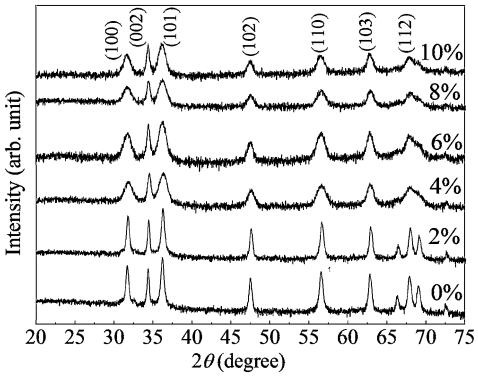

Fig. 1 XRD patterns of $Zn_{1-x}Co_xO$ nanorods ($x = 0$, 2%, 4%, 6%, 8%, 10%) with intensity on log scale

dripped into the former solution at RT under stirring until the precipitate was formed. The mixture was then transferred into a Teflon-lined autoclave (50 ml) and maintained at 393 K for 24 h. The products were collected and washed first with distilled water and then with alcohol, and finally dried at 393 K for 24 h.

The structures of samples were analyzed by X-ray diffraction (XRD) using a Cu Kα source with step size of 0.01°. The morphology and size were characterized by a transmission electron microscope (TEM, FEI Tecnai S20), and the purity of the samples were confirmed by the attached energy-dispersive X-ray spectrometer (EDS). The accuracy of EDS is dependent on the preparation of samples and test condition, etc., and it is within ±0.5% for our samples. No impurity ions other than O, Co, Zn, and C have been observed, indicating the high purity of our samples. The actual Co concentration in all $Zn_{1-x}Co_xO$ samples is measured by EDS, and close to the nominal concentrations, as shown in Table 1. For simplicity, we use a nominal concentration of Co to denote the samples, and the measured Co concentrations were used in the calculations. The magnetic properties were characterized by a physical property measurement system (PPMS, Quantum Design Inc.) at 300 K.

3 Results and Discussions

Figure 1 shows the XRD patterns of $Zn_{1-x}Co_xO$. All the diffraction peaks can be indexed into wurtzite ZnO (powder diffraction standard cards, JCPDS 36-1451) and no peak corresponding to any other impurity phase was observed, consistent with the EDS results. Table 1 shows that the lattice parameters calculated from the XRD data, which are a little smaller than those of pure ZnO, due to the smaller radius of Co ion (0.072 nm) than that of Zn ion (0.074 nm). In addition, it is noticeable that the variation of the lattice parameters with Co concentration is nonmonotonic, similar to the results reported by Xu et al. [13]. From the XRD patterns of $Zn_{1-x}Co_xO$, the width of diffraction peaks is almost identical when Co concentration is from 0% to 2%, and from 4% to 10%. But they are much narrower when Co concentration increases from 2% to 4%, indicating a sudden decrease of crystallinity. The grain size D of nanorods is calculated by the Debye–Scherrer formula:

$$D = 0.89\lambda/\beta\cos\theta \tag{1}$$

where λ is the wavelength of X-ray (0.154 nm), θ the Bragg angle of X-ray diffraction, β the FWHM (full width at half maximum) for the corresponding peak. Table 2 shows the grain size calculated from (100) and (002) peaks in all $Zn_{1-x}Co_xO$ and former are much smaller than latter. For each peak, the grain size changes slowly with Co concentration increasing from 0% to 2%, and from 4% to 10%. It changes abruptly when the Co concentration increases from 2% to 4%.

Figure 2 shows the TEM images of $Zn_{1-x}Co_xO$. For pure ZnO, some are elliptic and the others tend to be rodlike. They have wide size distribution with diameters of 20–100 nm and lengths of 40–200 nm. The size of $Zn_{0.98}Co_{0.02}O$ is not much different from that of ZnO, but the morphology is more likely to be rodlike. When Co concentration increases from 2% to 4%, $Zn_{1-x}Co_xO$ are mostly nanorods and their size are much smaller. The morphology does not change with further increasing Co concentration. They show diameters mainly around 10 nm and an aspect ratio of 2–5. With XRD results together, we can conclude that crystal grows along the c-axis direction and the Co concentration influences the grain size and morphology of ZnO prominently.

Figure 3 shows the M–H curves at 300 K for $Zn_{1-x}Co_xO$ nanorods. Pure ZnO nanorod is diamagnetic while $Zn_{1-x}Co_xO$ nanorods are all paramagnetic. But weak ferromagnetism can be seen in all $Zn_{1-x}Co_xO$ nanorods after the paramagnetic and diamagnetic contributions in high field are separated out [14].

Table 2 D calculated from (110) and (002) peaks of $Zn_{1-x}Co_xO$ nanorods ($x = 0$, 2%, 4%, 6%, 8%, 10%)

Co concentration (%)	0	2	4	6	8	10
D in the direction of (100) (nm)	37.4	37.4	9.0	8.7	9.0	9.8
D in the direction of (002) (nm)	46.2	49.1	22.4	27.1	23.8	23.8

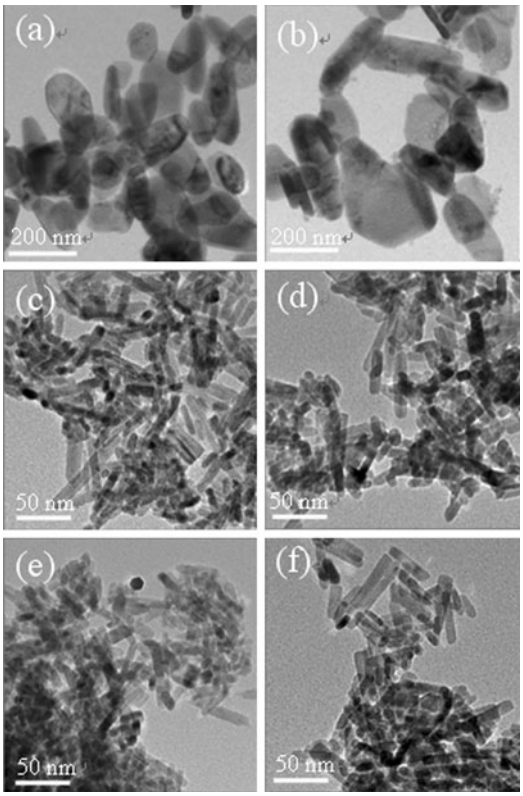

Fig. 2 TEM images of $Zn_{1-x}Co_xO$ nanorods ((**a**) $x = 0$, (**b**) 2%, (**c**) 4%, (**d**) 6%, (**e**) 8%, (**f**) 10%)

In order to analyze the influence of Co concentration on the magnetic properties of $Zn_{1-x}Co_xO$ samples, susceptibility χ of the samples is fitted by the method of least squares in high field ($H > 8000$Oe or$H < -8000$Oe). Susceptibility χ_{ZnO} measured in pure ZnO is negative, indicating the diamagnetic properties of bulk ZnO. χ in Co-doped ZnO has two contributions: diamagnetic susceptibility χ_{ZnO} for bulk ZnO and paramagnetic susceptibility χ_{Co} caused by doped Co. χ_{Co} is obtained by subtracting χ_{ZnO} from χ measured in all $Zn_{1-x}Co_xO$ nanorods at high fields. Figure 4 shows the variation of χ_{Co} with Co concentration. It can be seen that χ_{Co} almost increases with Co concentration linearly.

Magnetic moment μ_J per Co atom in $Zn_{1-x}Co_xO$ can be calculated from paramagnetic susceptibility χ_{Co}, the value is 3.2 μ_B/Co for the $Zn_{0.98}Co_{0.02}O$, 4.4 μ_B/Co for the $Zn_{0.96}Co_{0.04}O$, 4.1 μ_B/Co for the $Zn_{0.94}Co_{0.06}O$, 3.7 μ_B/Co for the $Zn_{0.92}Co_{0.08}O$, and 3.5 μ_B/Co for the $Zn_{0.90}Co_{0.10}O$, respectively. The substituted Co^{2+} ions might have two states, one with $L = 3$ and $S = 3/2$, and the other with $L = 1.07$ and $S = 3/2$, and the moment per Co is 4.1 μ_B/Co ($L = 1.07$, $S = 3/2$) or 6 μ_B/Co ($L = 3$, $S = 3/2$) [15]. The magnetic moment μ_J we get from $Zn_{1-x}Co_xO$ nanorods are very close to the former ($L = 1.07$, $S = 3/2$), which has been reported by Barla that the L/S is close 0.7 with $S = 3/2$ [10]. Thus, we can conclude that Co atoms are mainly isolated in $Zn_{1-x}Co_xO$ nanorods. The dispersive Co ions substituted Zn ions and the orbital moments were quenched by the crystalline field from the surrounding ZnO crystal lattice. The dominant interactions in $Zn_{1-x}Co_xO$ and $Zn_{1-x}Mn_xO$ samples are antiferromagnetic [7, 17]. The slight difference between the experimental and theoretical value of magnetic moment might be due to the weak antiferromagnetic interaction among the Co ions.

The ferromagnetic contribution in $Zn_{1-x}Co_xO$ nanorods can be clearly seen after subtracting the diamagnetic or paramagnetic contribution, as shown in the inset in Fig. 3. Though our XRD and EDS analysis has ruled out the secondary phase, we should be careful that there might be very faint traces of impurity phases under the detection limit. Knut et al. studied the possible impurities in Co-doped ZnO and concluded that $ZnCo_2O_4$ might be more stable than Co_3O_4, and $ZnCo_2O_4$ is expected to be nonmagnetic when n doped and ferromagnetic when p doped [17, 18]. However, the almost constant saturation magnetization of the ferromagnetic contribution with increasing Co concentration excludes the possible ferromagnetic contribution from $ZnCo_2O_4$. CoO is paramagnetic above the Néel temperature of 291 K and ferromagnetic behavior at 300 K might not be explained in terms of the formation of the CoO [19]. So, we can eliminate the effect of all these impurities. Furthermore, in the ZnO, powders prepared from the same chemicals by sol-gel method only exhibit diamagnetism at RT [20], excluding any other FM impurities from the source materials. Thus, the observed weak FM in $Zn_{1-x}Co_xO$ nanorods might not be due to the ferromagnetic impurities.

Figure 5 shows saturation magnetization (M_s) of the ferromagnetic contribution almost maintains in the same magnitude as that of pure ZnO when Co concentration increases from 2% to 10%, indicating that Co does not influence the FM in $Zn_{1-x}Co_xO$ nanorods. We can conclude the FM in $Zn_{1-x}Co_xO$ has the same origin as that in pure ZnO. The origin of FM was often considered to be from oxygen vacancies [6, 9] or defects on Zn sites [21] in ZnO. Barla has excluded the possible origin of FM from 3d electronic shells of the cations (Co and Zn in $Zn_{1-x}Co_xO$) [10]. Tietze suggested oxygen vacancies as the intrinsic origin for RT FM

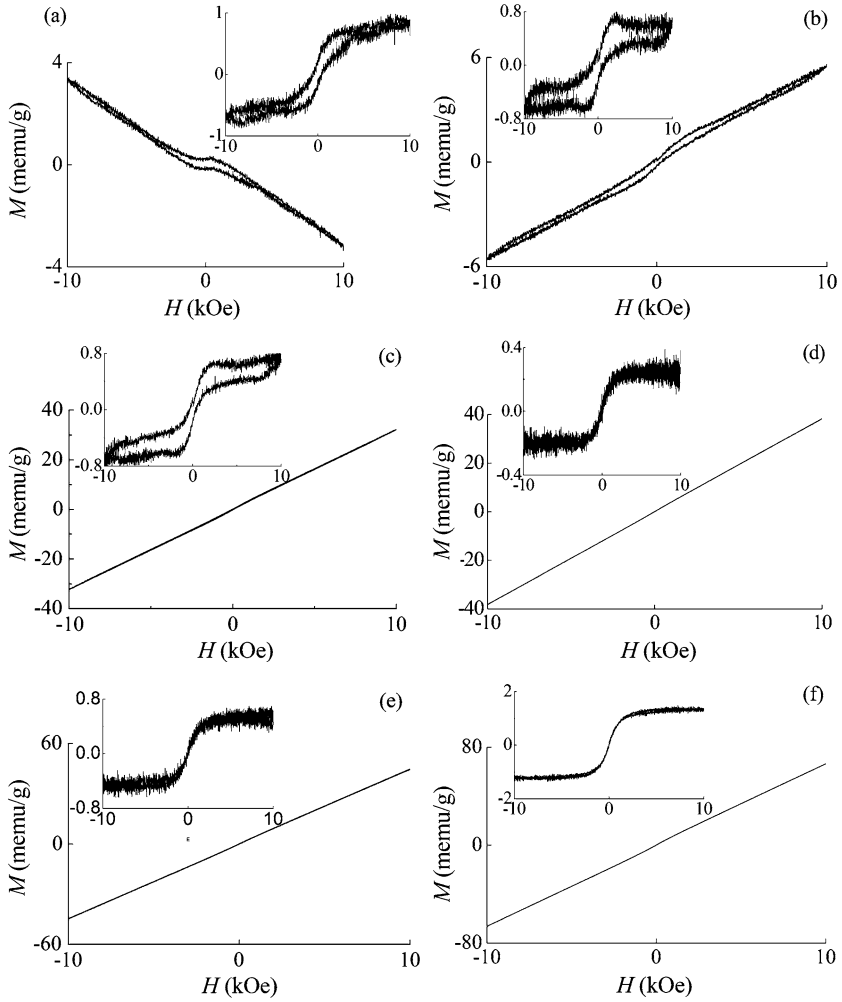

Fig. 3 M–H curves of $Zn_{1-x}Co_xO$ nanorods ((**a**) $x = 0$, (**b**) 2%, (**c**) 4%, (**d**) 6%, (**e**) 8%, (**f**) 10%). The *inset* shows the ferromagnetic contribution

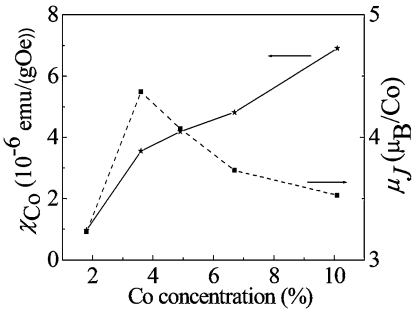

Fig. 4 The variation of χ_{Co} (*full curve*) and μ_J (*dotted curve*) with Co concentration

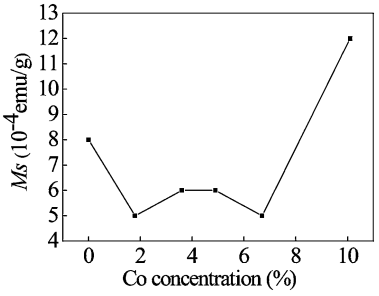

Fig. 5 The variation of saturation magnetization of the ferromagnetic contribution M_s with Co concentration

in doped ZnO [11]. Recently, Straumal reported that the FM originated from the vacancies locating at the grain boundaries above the threshold concentration [22]. This can be excluded since the single crystalline grain of our $Zn_{1-x}Co_xO$ nanorods. Sundaresan [23] found that FM is a universal feature of inorganic nanoparticles and it may be related to the surface FM of nanoparticles associated with point defects in DMS, which was confirmed recently by Khalid that ferromagnetic mass concentrated in the near-surface region related to defects [24]. Thus, the origin of FM observed here might be due to the large number of defects, e.g., oxygen vacancies or zinc vacancies, at the surface of nanoparticles.

4 Conclusions

$Zn_{1-x}Co_xO$ nanorods were synthesized at low temperature by the hydrothermal method. All the samples have good

crystallinity with preferential growth orientation along the c-axis without impurities. The particle shape changes from elliptic to rodlike and the particle size decreases abruptly with increasing Co concentration from 2% to 4% in $Zn_{1-x}Co_xO$. Pure ZnO is diamagnetic, while paramagnetism dominates $Zn_{1-x}Co_xO$ nanorods at room temperature. Magnetic moment μ_J per Co atom is close to the theoretical value of 4.1 μ_B/Co with $L = 1.07$ and $S = 3/2$ in all $Zn_{1-x}Co_xO$ nanorods, indicating that most Co atoms are isolated in $Zn_{1-x}Co_xO$ nanorods. All the samples exhibit weak FM; the saturation magnetization of the ferromagnetic contribution in $Zn_{1-x}Co_xO$ also maintains the same magnitude as that of pure ZnO with Co concentration increasing from 2% to 10%. We conclude that the weak FM in $Zn_{1-x}Co_xO$ might be due to the large number of defects, e.g., oxygen vacancies or zinc vacancies, at the surface of nanoparticles.

Acknowledgements The authors thank X.Y. Hu, J.S. Liu, and M.X. Xu for their help in the structural and magnetic measurements. This work is supported by the National Natural Science Foundation of China (50802041), National Key Projects for Basic Researches of China (2010CB923404), by NCET-09-0296, and Southeast University.

References

1. Ohno, H.: Science **281**, 951 (1998)
2. Dietl, T., Ohno, H., Matsukura, F., Cibert, J., Ferrand, D.: Science **287**, 1019 (2000)
3. Hsu, H.S., Huang, J.C.A., Huang, Y.H., Liao, Y.F., Lin, M.Z., Lee, C.H., Lee, J.F., Chen, S.F., Lai, L.Y., Liu, C.P.: Appl. Phys. Lett. **88**, 242507 (2006)
4. Liu, X.C., Shi, E.W., Chen, Z.Z., Zhang, H.W., Xiao, B., Song, L.X.: Appl. Phys. Lett. **88**, 252503 (2006)
5. Shi, T., Zhu, S., Sun, Z., Wei, S., Liu, W.: Appl. Phys. Lett. **90**, 102108 (2007)
6. Xu, Q., Zhou, S., Marko, D., Potzger, K., Fassbender, J., Vinnichenko, M., Helm, M.. Hochmuth, H., Lorenz, M., Grundmann, M., Schmidt, H., J. Phys. D, Appl. Phys. **42**, 085001 (2009)
7. Lawes, G., Risbud, A.S., Ramirez, A.P., Seshadri, R.: Phys. Rev. B **71**, 045201 (2005)
8. Liu, C., Yun, F., Morkoç, H.: J. Mater. Sci., Mater. Electron. **16**, 555 (2005)
9. Gacic, M., Jakob, G., Herbort, C., Adrian, H.: Phys. Rev. B **75**, 205206 (2007)
10. Barla, A., Schmerber, G., Beaurepaire, E., Dinia, A., Bieber, H., Colis, S., Scheurer, F., Kappler, J., Imperia, P., Nolting, F., Wilhelm, F., Rogalev, A., Müller, D., Grob, J.: Phys. Rev. B **76**, 125201 (2007)
11. Tietze, T., Gacic, M., Schutz, G., Jakob, G., Bruck, S., Goering, E.: New J. Phys. **10**, 055009 (2008)
12. Chu, D., Zeng, Y., Jiang, D.: Solid State Commun. **143**, 308 (2007)
13. Xu, X., Cao, C.: J. Alloys Compd. **501**, 265 (2010)
14. Singhal, R.K., Dhawan, M.S., Gaur, S.K., Dolia, S.N., Kumar, S., Shripathi, T., Deshpande, U.P., Xing, Y.T., Saitovitch, E., Garg, K.B.: J. Alloys Compd. **477**, 379 (2009)
15. Ney, A., Ollefs, K., Ye, S., Kammermeier, T., Ney, V., Kaspar, T.C., Chambers, S.A., Wilhelm, F., Rogalev, A.: Phys. Rev. Lett. **100**, 157201 (2008)
16. Rao, C.N.R., Deepak, F.L.: J. Mater. Chem. **15**, 573 (2005)
17. Knut, R., Wikberg, J.M., Lashgari, K., Coleman, V.A., Westin, G., Svedlindh, P., Karis, O.: Phys. Rev. B **82**, 094438 (2010)
18. Kim, H.J., Song, I.C., Sim, J.H., Kim, H., Kim, D., Ihm, Y.E., Choo, W.K.: Phys. Status Solidi B **241**, 1553 (2004)
19. Chu, D., Zeng, Y., Jiang, D.: J. Phys. Chem. C **111**, 5893 (2007)
20. Xu, Q., Zhou, S., Schmidt, H.: J. Alloys Compd. **487**, 665 (2009)
21. Hong, N.H., Sakai, J., Brizé, V.: J. Phys., Condens. Matter **19**, 036219 (2007)
22. Straumal, B.B., Mazilkin, A.A., Protasova, S.G., Myatiev, A.A., Straumal, P.B., Schütz, G., van Aken, P.A., Goering, E., Baretzky, B.: Phys. Rev. B **79**, 205206 (2009)
23. Sundaresan, A., Rao, C.N.R.: Nano Today **4**, 96 (2009)
24. Khalid, M., Setzer, A., Ziese, M., Esquinazi, P., Specmann, D., Pöppl, A., Goering, E.: Phys. Rev. B **81**, 214414 (2010)